

Performance Evaluation of ÇBİ Flotation Plant Using Mineralogical Analysis

Z. Ekmekçi, M. Can, Ş.L. Ergiın, Ö.Y. Gülsoy, H. Benzer & İ. B. Çelik
Hacettepe University, Mining Engineering Department, Beytepe - Ankara

ABSTRACT: Performance evaluation of ÇBİ Cu-Zn flotation plant was presented based on size-by-size materials balance and mineralogical analysis. Mineralogical analysis was performed mainly by using Clemex image analysis system and for some critical streams QemSCAN system. Although, the performance evaluation was performed for all of the streams in the plant, in this paper only the results of main streams were given for simplicity. The results revealed that finer grinding to prevent the loss of copper at +50 /ım fraction in combination with modification of flotation conditions to minimize the loss of valuables at -9 /ım size fraction would improve the performance of the flotation plant.

1. INTRODUCTION

Çayeli complex Cu-Zn sulphide ore deposit is situated in the North-East of Turkey. The concentrator treats a complex base metal ore having typical feed composition of 4.32 % Cu and 4.51 % Zn. The flotation feed is a mixture of yellow ore with high Cu content and black ore with high Zn content mined in the same region. The major sulphide minerals are pyrite, chalcopyrite and sphalerite associated with minor amounts of bornite, tennantite and galena (Akçay and Arar, 1998).

Performance of flotation concentrators need to be assessed both routinely and periodically to obtain maximum recoveries. Routine assessments are performed to monitor operations, and periodic assessments to evaluate performance and to identify processing problems. The assessment process involves collecting and analyzing representative samples and interpreting the data. The techniques used to analyse the samples are chemical and quantitative mineralogical analyses. Elemental recoveries are determined by materials balance performed throughout a circuit. When problems are indicated by the chemical assays and materials balance, a quantitative mineralogical analysis is needed for detailed interpretations (Petruk, 1992). Quantitative mineralogical data include mineral quantities, size distributions of free and locked

mineral grains, percentage of minerals that is liberated and locked.

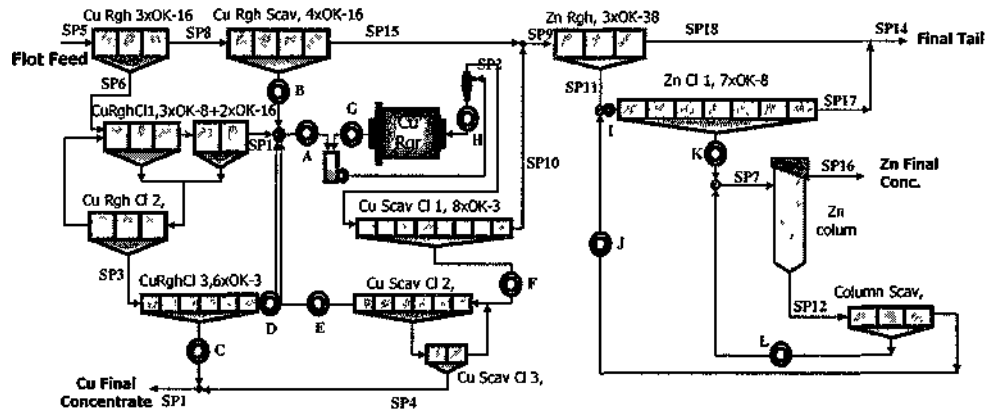
Performance of evaluation of the ÇBİ Cu-Zn flotation plant was performed by using chemical and quantitative mineralogical analyses. For this purpose a detailed sampling survey was performed in the copper and zinc flotation sections in the plant. Pulp samples from almost all of the streams were taken to determine performance of every stage in the flotation plant. However, in this paper, only the main streams were used in the performance analysis.

2.SAMPLING SURVEY

The sampling survey was undertaken at 148 dtph feed rate. The locations of the sampling points are illustrated in Figure 1. In the circuit, many streams were sampled by an automatic sampling system called multiplexer. The other flows were sampled by a specially designed sampling device. Before the sampling survey the operational parameters were monitored for 4-5 hours to ensure steady state operation during the survey. The sampling was performed sequentially four times over a period of two hours to obtain an adequate amount of representative samples.

Size distributions of the samples were determined by the combination of wet sieving and

cyclosizer down to 9 βm . The size fractions of +50 μm , -50+36 βm , -36+20 μm , -20+9 μm and -9 βm were prepared for chemical and mineralogical analysis.



SP : Samples from Multiplexer

Figure 1. Location of the sampling points.

3. MINERALOGICAL ANALYSIS

The bulk work was done using the Clemex optical image analysis system. Mineralogical analysis of the samples (excluding -9 μm fraction) were performed for all of the streams using Clemex image analysis system at Hacettepe University, Mining Engineering Department. In addition to that some of the critical samples were also analysed by the QemSCAN system at CSIRO, Australia.

3.1. Clemex System

Polished sections were prepared using 50 gr of representative samples. The samples were mounted in cold mounting resins and ground on the SiC discs with 400-, 600-, 1000- and 1200- mesh grain size. The ground samples were polished in three different steps by using the diamond abrasives with 3, 1 and 0.25 μm grain size.

Clemex Vision PE is the software program used for quantification of the images taken by an optical microscope equipped with a high resolution camera and motorized stage. Following image acquisition from polished sections, suitable algorithm instructions (a routine) are brought together in order to describe an image. A routine consists of a sequence of operations that are performed on each

image or field of analysis. The goal is to produce a representative binary detection of the microstructure and obtain meaningful measurements of a particular feature. The routine is built once on a typical field, and then it is repeated automatically by a motorized stage on any number of fields, generating results for the total area covered in the analysis. So it makes possible to perform the analysis on many numbers of features or particles.

3.2. Assay Reconciliation

As a check of the reliability of the measurements a comparison was made between the true chemical assay and the assays calculated from mineral modal analysis. QemSCAN identifies minerals on a chemical basis and accepted as the most reliable quantitative image analysis method. Comparison of the assays is shown in Figure 2. The excellent agreement shown confirms that QemSCAN is accurately identifying the mineral phases in the samples.

Comparison of the assays for Clemex system is shown in Figure 3. The results showed that the mineral phase identification is quite good, but not as accurate as QemSCAN. This was related to the segmenting of the optical image, which is always

more difficult than a SEM image. But in general the results are reasonable for sound interpretation.

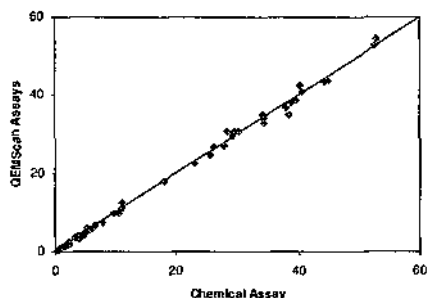


Figure 2. Comparison of the chemical assays performed with standard Atomic Absorption Spectroscopy (AAS) and QEMScan methods.

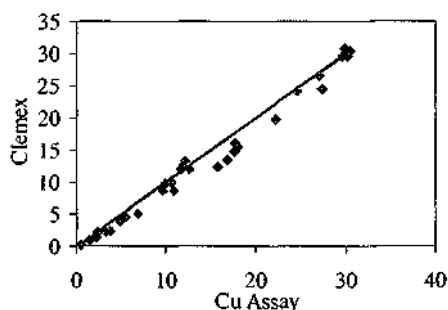


Figure 3. Comparison of Cu assay measured by standard AAS method and calculated from Clemex system.

4. MASS BALANCING

In any sampling operation, some errors are inevitable due to dynamic nature of the system, the physical conditions at a particular point, random errors, measurement errors and human errors. Mass balancing involves statistical adjustment of raw data to obtain the best fit estimates of flowrates.

During sampling surveys, excess data were collected in some points to obtain reliable solution in mass balancing. After having Cu, Zn and Fe assays of the samples, mass balancing studies were commenced. Using mass flow rate of the fresh feed and chemical assays of the streams, flowrates and recoveries of copper, zinc and pyrite in each stream were calculated. Mass balancing studies were carried out by using a step by step approach around various nodes and finally for the whole flotation plant. Therefore, the calculations were checked and verified for different routes (Convergence limits in

all iterations were chosen as 10'. Mass balancing of the raw data was performed by using JKSimMet software). The accuracy of the mass balancing is shown in Figure 4 by plotting raw assays vs adjusted assays.

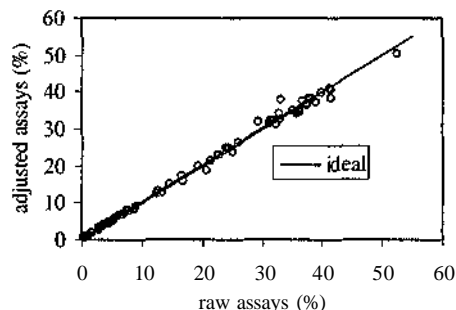


Figure 4. Overall comparison of the raw and adjusted assays.

5. RESULTS AND DISCUSSION

In spite of mineralogical evaluations have been done for all of the streams in the flotation plant, in this paper only the results of the main streams are discussed due to complexity of the circuit.

5.1. Size by Size Recovery and Metal Distribution

In this section, the overall flotation performance of the entire circuit is discussed based on the characteristics of the flotation feed, copper final concentrate, zinc final concentrate and final tail. The mass flow rate, recovery and assays of copper, zinc and pyrite are illustrated in Figure 5.

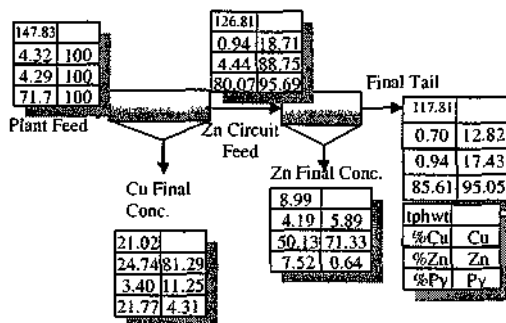


Figure 5. Overall performance of the flotation operation.

For the whole copper circuit, it is not possible to calculate size by size recovery based on the plant feed, the copper final concentrate and the zinc rougher feed, due to the copper regrinding (Figure 1). Therefore, using mass flowrates and mass balanced size by size data for the copper final concentrate and copper circuit tail (zinc rougher feed), a reconstituted feed (virtual feed) for the copper circuit was calculated. Then, size by size recovery in the copper circuit was calculated using the virtual feed. The comparison of Cu metal distribution in the plant feed and the virtual feed is shown in Figure 6. As expected, copper exists in +36µm decreased in the virtual feed, and the amount of copper increased in -20/µm. Therefore, using virtual feed in place of plant feed provided real recovery figures.

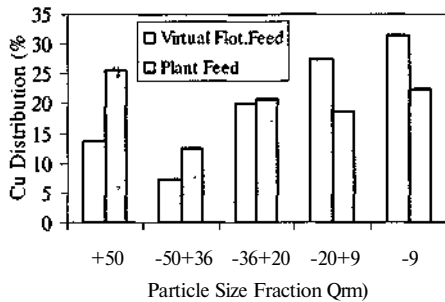


Figure 6. Comparison of Cu distribution between the virtual feed and the plant feed.

The size-by-size recovery of copper and copper distribution of the streams is presented in Figure 7. The copper recovery and grade of the copper final concentrate are 81.29 % and 24.74 % Cu, respectively (Figure 5). However, size-by-size copper recoveries to the copper final concentrate showed that the recovery values in +50/µm and -50+36/µm were as low as 29% and 65%, respectively. As can be seen from Cu metal distribution data, +50/µm fraction contained 46% of the copper loss to the Zn circuit feed and 41% of the copper in the final tail. Therefore, considering the 18.71% total copper loss to the final tail and zinc concentrate (Fig. 5), it was found that 8.6% of the total copper loss was in the +50/µm fraction. Most of the copper lost to the zinc circuit feed at this size fraction reported to the final tail.

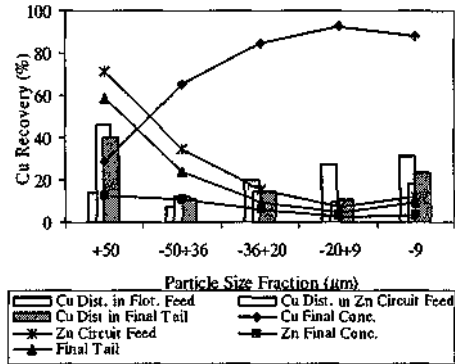


Figure 7. Size-by-size copper recovery of the main streams and Cu metal distribution in the plant feed and Zn circuit feed in ÇBI flotation plant.

The size-by-size recovery of zinc and zinc distribution of the streams are presented in Figure 8. The recovery and grade of the zinc final concentrate were 71.33 % and 50.13% respectively (Figure 5). Figure 8 shows that the recoveries in the coarse (+50 µm) and fine (-9 µm) particle fractions are substantially lower than the medium size range. The majority of zinc loss occurred at these size fractions. Zn distribution in the final tail showed that these fractions contained 2/3 of the Zn. The zinc lost to the copper concentrate increases as the particles size decreases. Considering the total 11.25 % Zn loss to the copper final concentrate (Fig 5), 10.65% of the Zn lost was due to -36µm fractions.

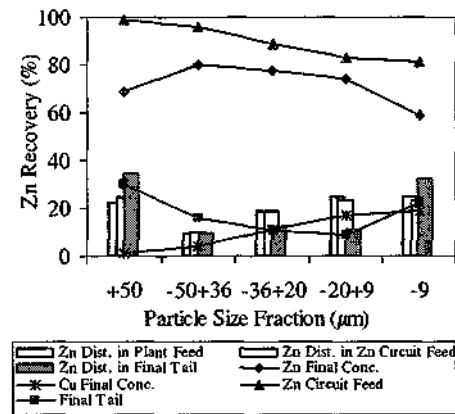


Figure 8. Size-by-size zinc recovery of the main streams in ÇBI flotation plant.

5.2. Mineralogical Evaluations of the Main Streams

Plant Feed

The results of mineralogical analysis of the plant feed are given in Figure 9 as a function of particle size fractions. It must be noted that mineralogical analysis of -9 *fm* fraction has not been performed and hence this fraction is not included in the graph. However, liberation state of -9 *fm* fraction was assumed to be similar to the -20+9 *fm* fraction. Figure 9 shows that about 55 % of the plant feed is composed of liberated pyrite particles, mainly at -36 *fm* fraction. The total liberation of both chalcopyrite and sphalerite was about 75% (liberation of -9 /*tm* fraction assumed as the same with -20+9/*tm* fraction). The locked chalcopyrite particles are mainly found with pyrite rather than sphalerite. Besides, the locked chalcopyrite/pyrite particles are mostly accumulated in -36 /*tm* fraction. Similar behaviour is also observed with sphalerite/pyrite particles.

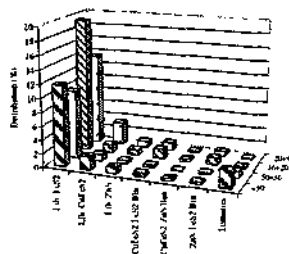


Figure 9. Modal analysis of the flotation feed for different size fractions.

The amount of ternaries in the +50 *fm* and -50+36 /*tm* fractions is considerably higher than the finer fractions. In spite of that the amount of chalcopyrite/pyrite, chalcopyrite/sphalerite and sphalerite/pyrite binary particles is very low compared to the ternaries in these fractions. Mineral distribution of the ternary particles in +50 *fm* and -50+36 *fm* fractions are also calculated and illustrated in Figure 10. The results show that the amount of pyrite in both fractions is higher than chalcopyrite and sphalerite, particularly in -50+36 *fm* fraction. Chalcopyrite occupies larger area than sphalerite, indicating that majority of these particles may be considered as chalcopyrite/pyrite binary particles with small inclusions of sphalerite. Considering the higher percentage of pyrite and

coarse size, these particles can be liberated by finer grinding of the flotation feed.

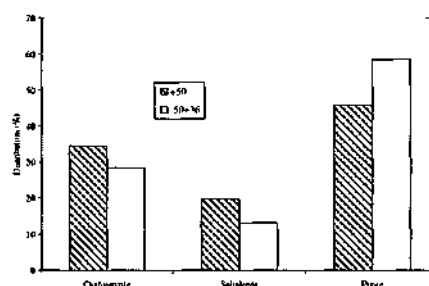


Figure 10. Mineral distribution of the ternary particles at +50 /*im* and -50+36 *fm* fractions of plant feed.

Copper Final Concentrate

The fine sphalerite particles are considered to be recovered mainly by entrainment and the coarse particles in the form of locked particles with chalcopyrite, as the flotation conditions were not suitable for flotation of sphalerite. Di-isobutyl dithiophosphinate, a selective collector for copper minerals, was used as collector in strongly alkaline condition (>pH 11.5). In these conditions liberated sphalerite and pyrite particles were considered to report to the copper concentrate by entrainment.

Mineralogical analysis of the copper final concentrate showed that liberation of the chalcopyrite was 81.55% (liberation of -9 *fm* fraction assumed as the same with -20+9/*tm* fraction) (Figure 11). More than 30 % of these particles are found at -36 *fm* fraction. In addition to that considerable amount of chalcopyrite-pyrite and chalcopyrite-sphalerite binary particles are also recovered to the copper final concentrate. Therefore, the large portion of pyrite and sphalerite recovered to the concentrate are in the form of locked particles. Besides, very fine pyrite particles (-20 *fm*) are also recovered most probably by entrainment. The mineralogical analysis of the copper final concentrate clearly shows that finer grinding is required to decrease the amount of pyrite and sphalerite at -36 /*tm* fraction. However, it must be noted that in the case of fine regrinding, the flotation conditions must be suitable for fine particle flotation, in terms of both improving flotation of -9 *fm* chalcopyrite particles and minimizing entrainment of fine pyrite and sphalerite particles.

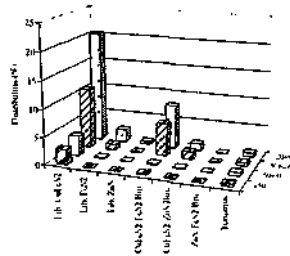


Figure 11. Modal analysis of copper final concentrate for different size fractions.

The amount of ternary particles in the final concentrate is substantially lower than the other mineral components. Moreover, the mineral distribution of the ternary particles shows that the majority of these particles consist of chalcopyrite (Figure 12).

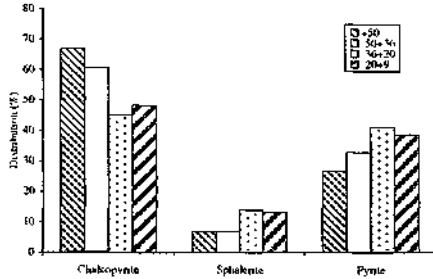


Figure 12 Mineral distribution of the ternary particles of copper final concentrate at different particle size fractions.

Mineral distribution of chalcopyrite/pyrite and chalcopyrite/sphalerite binary particles at -36+20 /im and -20+9 /im are also illustrated in Figures 13 and 14. It appears that zinc loss occurs from the ternary particles and chalcopyrite/sphalerite binary particles at fine particle size range. It is very difficult to liberate the fine ternary particles due to very low sphalerite content. In addition to that there are some losses in the form of fine liberated sphalerite particles, most probably due to entrainment. It must be born in mind that the -9 /im is not taken into account in the mineralogical analysis and the fact that very fine liberated sphalerite particles are recovered at higher levels than the next coarse fraction as shown in Figure 8. Therefore, higher amount of very fine liberated sphalerite particles are anticipated to be one of the main source of zinc loss to the copper final

concentrate. Therefore, the cleaning process must be performed carefully to lower the entrainment of fine particles of sphalerite and pyrite.

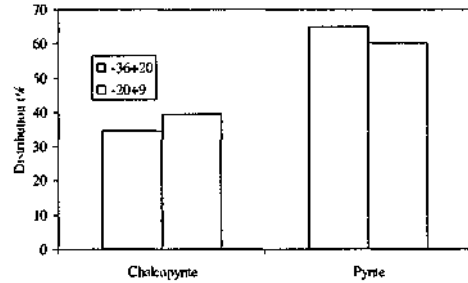


Figure 13. Mineral distribution in chalcopyrite/pyrite binary particles at -36+20 and -20+9 /im particle size fractions of copper final concentrate.

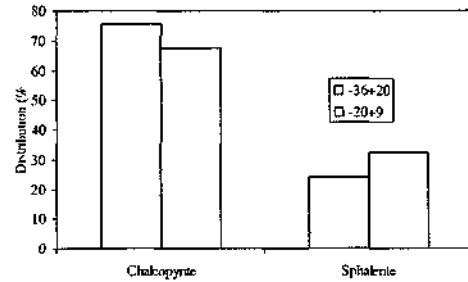


Figure 14. Mineral distribution in chalcopyrite/sphalerite binary particles at -36+20 /im and -20+9 /im particle size fractions of copper final concentrate.

Zinc Final Concentrate

The results of the mineralogical analysis of the zinc final concentrate showed that sphalerite liberation was 86.74% (liberation of -9 /im fraction assumed as the same with -20+9/im fraction). Very small amount of chalcopyrite is recovered in the form of liberated particles, mainly at coarse size fractions (Figure 15). These coarse liberated chalcopyrite particles could not be recovered in the copper circuit most probably due their slow flotation kinetics and/or insufficient residence time.

However, the loss of chalcopyrite appears to be also from the binary and ternary particles. Mineral distribution of the ternary particles is given in Figure 16. More than 50 % of the area of +36 /im particles is sphalerite and 20 % chalcopyrite. This type of mineral composition makes them floatable

in the existing chemical conditions. As the particle size decreases the percentage of pyrite in the ternary particles increases. Pyrite is mainly recovered with the locked particles and to some degree at very fine size due to entrainment.

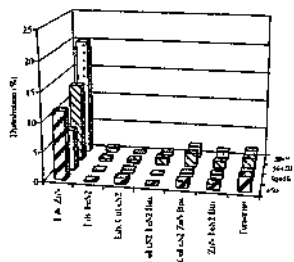


Figure 15. Modal analysis of zinc final concentrate.

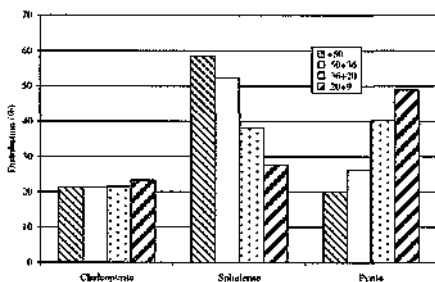


Figure 16. Mineral distribution of the ternary particles at various fractions of zinc final concentrate.

The mineral distributions of chalcopyrite/pyrite and chalcopyrite/sphalerite binary particles at 36+20 /*tm* and -20+9 /*im* fractions are given in Figures 17 and 18 respectively. The area percentage of chalcopyrite in chalcopyrite/pyrite binary particles is about 20 % for both size ranges. This value increased to about 30 % in the chalcopyrite/sphalerite particles. It must be noted that these binary particles are mainly in fine size range and these particles must be removed in the copper circuit, possibly by regrinding and more efficient fine particle flotation.

Final Tail

When pyrite was included, the liberation state of the other minerals is not clearly illustrated due to large amount of pyrite in the final tail. More than 70 % of the tailing stream (-9 *fixa* is not included) consists of liberated pyrite particles mainly at -36 /*tm* fraction.

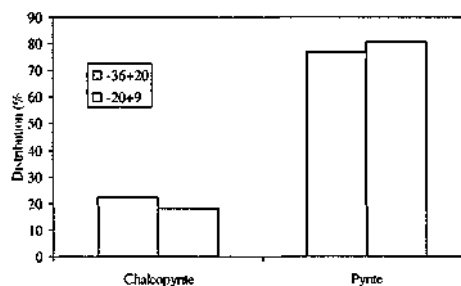


Figure 17. Distribution of chalcopyrite and pyrite in chalcopyrite/pyrite binary particles in -36+20 /*tm* and -20+9 /*im* fractions of zinc final concentrate.

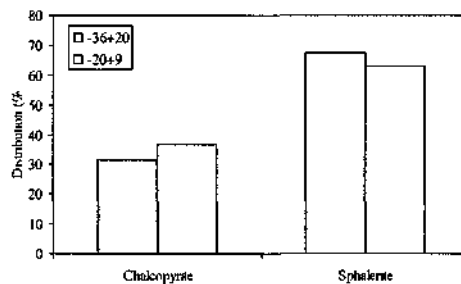


Figure 18. Distribution of chalcopyrite and pyrite in chalcopyrite/pyrite binary particles in -36+20 /*tm* and -20+9 /*im* fractions of zinc final concentrate.

Therefore, the liberation state of chalcopyrite and sphalerite are illustrated without liberated pyrite in Figure 19. The liberation of chalcopyrite and sphalerite were 28.32 and 46.28%, respectively (liberation of -9 /*tm* fraction assumed as the same with -20+9/*im* fraction). The coarse particles reported to the tailings are generally in the form of locked particles with slow floatability. The copper loss is mainly in the form of chalcopyrite/pyrite binary particles at -36+20 /*im* and -20+9 /*im* fractions and ternary particles at +50 /*im* and -50+36 /*im* fractions. As it was explained above, the reason for the measurement of high percentage of ternary particle in the coarse size fractions may be due to the high sensitivity of QemScan, which has the ability to detect very small inclusions of either sphalerite or chalcopyrite. However, it appears from Figure 20 that the ternary particles contain mainly pyrite. The chalcopyrite and sphalerite contents are higher in +50 /*im* fraction than the finer fraction. Therefore, the zinc loss to the final tailing from +50 /*im* fraction (Figure 9) is mainly from the ternary

particles and to a lesser degree from sphalerite/pyrite binary particles.

difficult and are reported to the final tail. But they are suitable to liberate by finer grinding due to very high content of one mineral (pyrite) (Petruk, 1992).

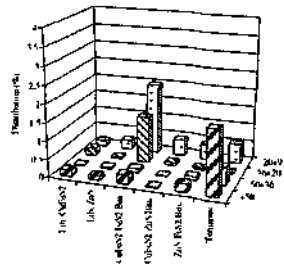


Figure 19. Modal analysis of the final tail in the absence of pyrite.

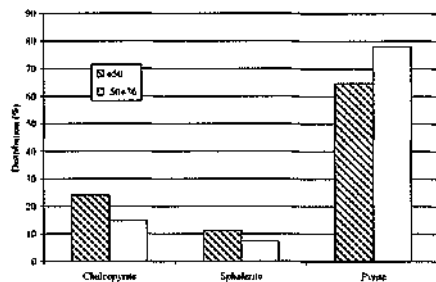


Figure 20. Mineral distribution of the ternary particles at +50 μm and -50+36 μm fractions of final tail.

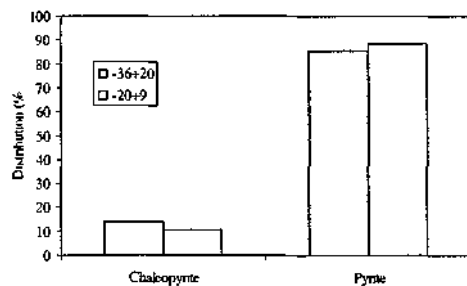


Figure 21. Distribution of chalcopyrite and pyrite in chalcopyrite/pyrite binary particles at -36+20 μm and -20+9 μm fractions of final tail.

Chalcopyrite is also lost with chalcopyrite/pyrite binary particles finer than 36 μm. Distribution of chalcopyrite and pyrite in these particles is given in Figure 21. These particles contain even less than 10 % chalcopyrite which makes their flotation very

6. CONCLUSIONS

The main copper loss was from +50/μm fraction. The recovery of +36/μm fraction was significantly lower than the others. Therefore, it can be concluded that finer flotation feed would improve the performance of the copper circuit. Zinc reported to the copper final concentrate is in the fine size ranges and recovered mainly by entrainment. For the locked particles, very fine regrinding is necessary. This should be applied with caution due to possibility of losing copper through very fines.

In the zinc circuit, the losses were from -9/μm and +50/μm fractions. Finer flotation feed would also decrease losses through +50/μm. However, further studies to improve -9/μm recovery are required.

Acknowledgement

The authors gratefully acknowledge technical and financial support of Çayeli Bakır İşletmeleri A.Ş.

REFERENCES

- Akçay, M and Arar, M., 1998; Geology, mineralogy and geochemistry of the Çayeli massive sulphide ore deposit, Rize, NE Turkey. *Mineral Deposits: Processes to Processing*, (Ed. Stanley et al.), Balkema, Rotterdam, 459-462.
- Petruk, W., 1992; Applied mineralogy and materials balancing procedures. Evaluations of flotation concentrators. *Innovations in Flotation Technology*, NATO ASI Series, Vol 208, Kluwer Academic Publishers, 125-148.